Journal of Laser Applications

Experimental investigation of temperature field, defects, and mechanical strength in dissimilar laser bonding of Ti6Al4V and polyethylene terephthalate

Cite as: J. Laser Appl. **33**, 012038 (2021); https://doi.org/10.2351/7.0000275
Submitted: 09 November 2020 . Accepted: 15 December 2020 . Published Online: 06 January 2021

Junyao Xue, Mohammad Hossein Razavi Dehkordi, Ali Abdelahi, Adel Abdelahi, Ehsan Rasti, and Zhixiong Li

Journal of Laser Applications ARTICLE scitation.org/journal/jla

Experimental investigation of temperature field, defects, and mechanical strength in dissimilar laser bonding of Ti6Al4V and polyethylene terephthalate

Cite as: J. Laser Appl. 33, 012038 (2021); doi: 10.2351/7.0000275
Submitted: 9 November 2020 · Accepted: 15 December 2020 ·
Published Online: 6 January 2021

Junyao Xue,[1] Mohammad Hossein Razavi Dehkordi,[2] Ali Abdelahi,[2] Adel Abdelahi,[2] Ehsan Rasti,[3,a)] and Zhixiong Li[1]

AFFILIATIONS

[1]Hubei Key Laboratory of Power System Design and Test for Electrical Vehicle, Hubei University of Arts and Science, Xiangyang 441053, China
[2]Department of Mechanical Engineering, Najafabad Branch, Islamic Azad University, Najafabad, Iran
[3]Department of Mechanical Engineering, Sarvestan Branch, Islamic Azad University, Sarvestan, Iran

[a)]**Author to whom correspondence should be addressed; electronic addresses:** rasti@iausarv.ac.ir. **Telephone:** 989173870805

ABSTRACT

Laser welding is one of the most common technologies with various applications in different industries. In this paper, laser joining of the Ti6Al4V alloy and polyethylene terephthalate (PET) as a means of two common materials is discussed. According to the experimental results, the focal length is a very important parameter in this dissimilar laser welding, and because of the low melting point of PET, it is not possible to create welding at low focal lengths. Furthermore, changing the welding parameters such as welding speed and pulse duration changes the temperature field of the molten pool and its surrounding points, as well as the number, distribution, and the shape deformation of the bubbles formed in PET, which plays an important role in welding quality and mechanical strength. The number of bubbles clearly has a significant influence on the surface contact area and the resultant shear load test values. Generally, reducing the surface contact area between PET and the Ti6Al4V alloy evidently reduces the tensile shear load of the joints. The shear load of the joints has had about 40% variation upon changing the focal length. Additionally, the shear load changed only about 10% by changing the pulse duration from 6 to 10 ms. Seemingly, changing the energy density through a variation of focal length has had a higher influence of about 30% than the incident time of laser beam through increasing the pulse duration. Apart from selecting different laser parameters, the measured temperature in ranges between 100 and 120 °C can produce acceptable joints with lower defects.

Key words: laser welding, titanium alloy, polyethylene terephthalate (PET), shear load, mechanical strength

I. INTRODUCTION

Applications of lasers have enhanced in various industries. Gu *et al.*[1] investigated the effects of laser scanning strategies on selective laser melting of pure tungsten. Their results showed that pores and cracks were the main defects in selective laser melting (SLM)-processed tungsten parts. Also, compared with other scanning strategies, a compressive strength of 923 MPa with an elongation of 7.7% was obtained. Djogo *et al.*[2] presented techniques to demonstrate the potential for 3D writing of high-density optical packaging components, for efficiently connecting optical fibers to silicon photonic (SiP) processors for use in telecom and data centers. Their finding illustrated that a 3D waveguide fan-out design provided an attractive balancing of low losses, high channel density, modematching, low cross talk, and compact footprint. The 3D additive and subtractive processes, thus, demonstrated the potential for higher scale integration and rapid photonic assembly

for telecom interconnects. Tino *et al.*[3] presented a review of clinical practice, emerging trends, and research opportunities using additive manufacturing (AM). They surveyed the key advantages of AM in radiotherapy where rapid prototyping allows for patient-specific manufacture and investigated how current AM processes are exploited by researchers to achieve patient tissuelike imaging and dose attenuations. In recent years, similar to laser welding, the benefits of laser processing are being recognized and exploited to produce better products with higher quality and lower cost. The heat required for welding is supplied by a tightly focused light beam with a diameter as small as two-thousandths of an inch. Today, different types of industries such as the electronics industry and the automotive industry are placing increased requests for direct laser joining of polymer-metal materials for many applications.[4–14] One of the metals used for laser welding is titanium alloy. The advantages of titanium alloy for welding include a low conductivity heat transfer coefficient and a low thermal expansion coefficient; they cause less heat loss and lower stress during welding. These characteristics make titanium an attractive material for welding. Mian *et al.*[15] studied defects in laser bonding of titanium and polyimide for medical applications. They can also predict the bond strength effect on the mechanism of failure. Gui *et al.*[16] investigated the double-sided laser welding of dissimilar titanium alloys with linear changeable thickness and the overlap rate effects on porosity formation. Double-sided laser welding parameters are optimized in this study. In an experimental study, the laser welding joining of NiTi alloy to Ti6AL4V was studied on a 1 mm thick plate with different heat inputs to control the cooling rate. By utilizing a Yb fiber laser, dissimilar butt joints quality of NiTi to Ti6Al4V was optimized. In the fusion zone, a fine dendritic structure was revealed.[17]

Today, researchers focus on melt pools and temperature field analysis for achieving better laser welding performance. Pouquet *et al.*[18] studied the molten pool and the structure of stainless steel and NiTi alloy under laser welding. They found that the geometry of the weld depends on the welding parameters and the material's thermal properties. Balasubramanian[19] used silver as the middle layer welding of titanium grade 5 and stainless steel. They examined the temperature field and the influence of various parameters on the quality of the welding and indicated that the bonding temperature had a greater influence on the shear strength of the layers than the pressure and holding time. Tan *et al.*[20] used scanning electron microscopy and transmission electron microscopy to study the structure of magnesium and stainless steel after laser welding and described the effects of welding speed and heat input. The bonding of ferritic stainless steel and titanium was investigated by applying a nickel layer by Yıldız *et al.*[21] The increasing temperature, pressure of the experiments, and the microstructure and hardness of the sample were studied. Zhang *et al.*[22] concluded that laser welding of titanium alloy and stainless steel using a copper sheet as the interlayer caused an inhomogeneous distribution of hardness in the weld. These results were obtained by performing tensile and nanoindentation experiments. An inhomogeneous distribution occurred due to the composition of the solid copper solution in the melt pool and the mechanical properties were improved by it. The influence of the pulsed laser beam incident angle on melt pool geometry, microstructures, and the elongation of weld joints was investigated by Kumar *et al.*[23] They studied stainless steel sheet bonding by butt welding and robotic control. The effects of welding parameters such as the welding speed, power, and incident angle of the laser beam on the ultimate tensile strength were determined by conducting experiments. The experiments revealed that the metal obtained from the incident angle of 85.5 had the highest tensile strength and quality. Mai and Spowage[24] investigated the welding sound produced by laser welding. They used combinations of three different materials and pulsed Nd:YAG laser. They showed that the melting ratio of controlling metals is a significant parameter for the welding of dissimilar metals. Heat distribution is controlled and joining material interaction is minimized in laser welding because of high power density and energy input limited locally.

Time control of temperature distribution is necessary inside irradiated materials when attempting to optimize the laser welding process.[25] In a numerical and experimental study of laser welding, Akbari *et al.*[26] investigated the temperature distribution, heat affected zone (HAZ), and shape of the molten pool on titanium alloy. They also used the heat field to predict the molten pool's dimensions. The numerical and experimental results were in good agreement, and the thermal model prediction error was about 2%–17%. The welding speed has a direct impact on the temperature distribution and has reached to the highest point of the temperature at longer time. Frewin and Scott[27] simulated a three-dimensional laser welding using the finite element model and showed that their suggested model was quite sensitive to the absorptivity of the laser beam and energy distribution. Kong *et al.*[28] predicted temperature distribution caused by heat generated from a direct diode laser. They used the finite element model and the method of Monte Carlo to calculate the history of temperature as thermal loading to evaluate the growth of grains in the HAZ of dual-phase steel DP980. They demonstrated that the gradient of temperature in the HAZ is reduced by the enhanced laser beam's scanning speed under a laser power of 2 kW.

Faraji *et al.*[29] investigated the effects of welding speed, laser power, and welding current on the characteristics of weld pool and shape in hybrid laser-TIG welding of aluminum alloy by using an experimental and numerical method. Heat transfer and fluid flow were simulated in the melt pool by using a numerical method, and the weld shape was studied for various welding conditions. The results demonstrated that upon reducing the welding speed and increasing the welding current and laser power, the buoyancy and Marangoni forces increased. They presented a model that could well predict the weld geometry.

Fluid flow details and heat transfer to the weld pool from the laser keyhole played a major role in specifying the weld size and shape. Abderrazak *et al.*[30] utilized the experimental and numerical methods to study the thermal phenomena for laser keyhole welding. They carried out experiments to investigate the laser welding effects on the melt pool sizes; they used a three-dimensional finite volume model to simulate melt pool formation and keyhole. The result showed that the parameters of welding such as the incident laser power and welding speed had an influence on the size and shape of the molten pool.

The dimensions of the weld cross section profile have been quantitatively studied through numerical and experimental analysis.

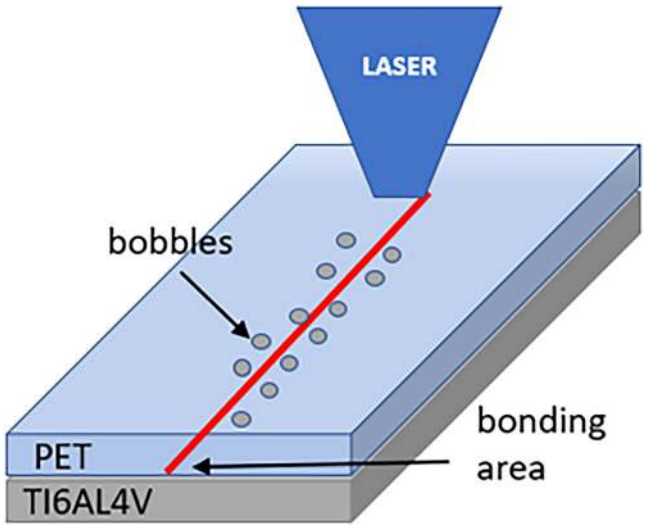

FIG. 1. Schematic of the welding configuration.

It is very difficult to measure the temperature in the molten pool, and temperature distribution is simulated through a numerical method. Then, the size of the HAZ region and melt pool profile was calculated using temperature distribution. Akbari *et al.*[31] used the numerical method for calculating the cooling rate in the molten pool and showed that the weld center point was the suitable location for cooling rate and martensitic transformation in the zones of weld fusion. Jiang *et al.*[32] investigated the distribution of asymmetric temperature in moving titanium alloy exposed to concentrated laser welding. They carried out a numerical simulation to solve the governing equations by considering the initial and boundary conditions and the numerical simulation results validated by the experimental outputs. The results demonstrated that increasing the size of the melt pool was more effective than decreasing the diameter of the laser pulse. Laser beam welding of the Ti6Al4V sheet was simulated by Azizpour *et al.*[33] The molten pool dimensions were calculated by using the numerical method and validated with the experimental data. The results showed that the numerical results were in good agreement with the experimental data.

Many research studies have been performed on laser welding of metals and polymers. In studies on laser welding, the welding of metals and polymers was investigated separately. The temperature field and the size of the melt pool were studied for homogeneous and inhomogeneous metals of different thicknesses. However, only a limited number of research studies have focused on metal and polymer welding. In this study, dissimilar pulsed laser welding of titanium alloy (Ti6Al4V) and PET are performed. Due to the importance of the temperature field and the molten pool changed by welding parameters, the temperature field and the quantity and dimensions of the created bubbles in the molten pool are ascertained and examined.

II. EXPERIMENTS

In the laser welding of the PET plate and Ti6Al4V alloy, it should be noted that transparency of PET can pass light; it is placed on top, with the Ti6Al4V alloy being placed under the PET plate, as shown in Fig. 1. Thus, the laser beam passes through the PET sheet and hits the Ti6Al4V alloy, generating a molten pool at a place between the PET sheet and the Ti6Al4V alloy. Moreover, following the creation of the molten pool, heat transfers from the Ti6Al4V surface to the PET sheet and results in melting, creating bubbles, and there is apparent shape deformation of PET. Thus, because of the heat generation between materials, the PET plate and the Ti6Al4V alloy are jointed.

Using a high laser power and welding in the focal length of the laser beam creates a high energy density, which intensively melts and evaporates PET as it has a low melting point. Therefore, as working parameters, a lower power and a higher focal distance than typical metal welding parameters were used to avoid

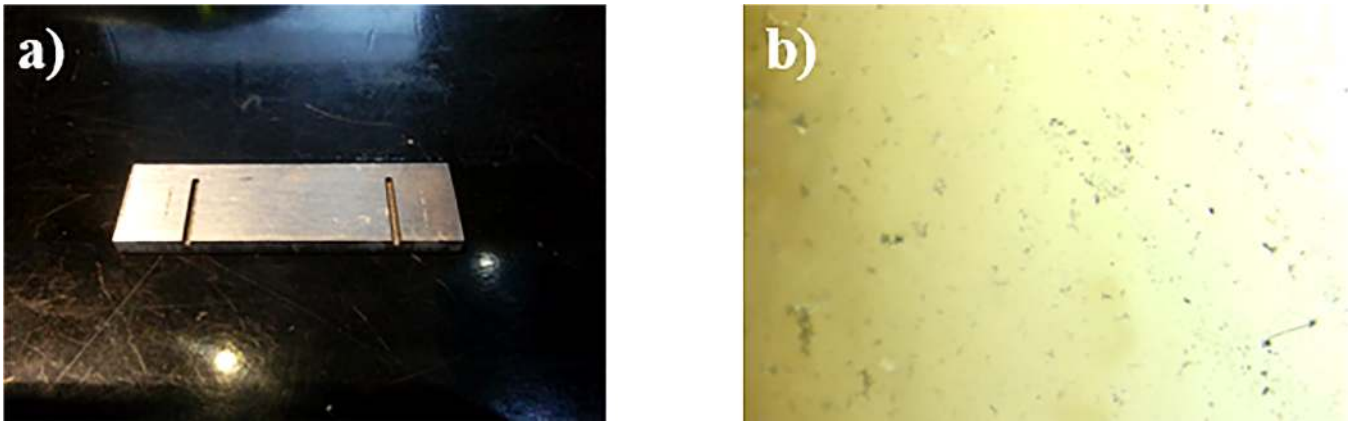

FIG. 2. (a) Titanium workpiece with 2 mm thickness and (b) PET sheet with 0.7 mm thickness.

PET evaporation and create an appropriate molten pool in the TiAl4V alloy.

As can be seen in Fig. 2(a), Ti6Al4V plates with dimensions of 50 mm length, 30 mm width, and a thickness of 2 mm were prepared. Two grooves with a depth of 1.1 mm were applied 3 cm from each other and 1.5 cm from the center to place the thermocouple. Also, PET plates with dimensions of 50 mm length, 30 mm width, and a thickness of 0.7 mm were cut and prepared, as shown in Fig. 2(b).

An Nd:YAG IQL-10 pulsed laser with 450 W peak power and 1.06 μm wavelength was employed. The pulse duration (the time during which the pulse is on), pulse frequency, and pulse energy ranges of 0.2–0.25 ms, 1–250 Hz, and 0–40 J were selected, respectively. Argon gas was used for weld protection. Thermocouples are required to record the temperature variations. Thus, thermocouples of type K with a length of 10 cm, a diameter of 1 mm, an operating temperature range of 40–1260 °C, and an accuracy of $\pm$1% were applied. The thermocouples were placed in a groove on the Ti6Al4V alloy at a transverse distance of 2 mm from the molten pool's center. An Advantech USB4718 data acquisition card was utilized to record temperature changes in laser welding. Metallography was carried out on the samples to investigate the weld microstructure and grains formed in the base metal and welded location. Preparing the welded sample's surface, which was done by polishing the surface, is an important prerequisite in metallography. The welded samples were mounted by using standard metallography methods (sanding with sizes of 200, 400, 600, 800, and 1000 grit) and polished. Then, they were etched in the curl solution consisting of 91 ml of distilled water, 6 ml of nitric acid, and 2 ml of hydrofluoric acid. Images were taken from the microstructure by using an ATSM E 883-17 microscope.

III. RESULTS AND DISCUSSION

In this section, the effects of pulsed laser parameters (e.g., focal length, welding speed, and pulse duration) during the process of laser welding were investigated. The temperature near the melt pool and molten pool microstructure and the dimensions in the Ti6Al4V alloy were measured. The number of created bubbles and the size of HAZ in the PET were analyzed as well. The different laser parameters used in the experiments are given in Table I.

TABLE I. Parameters of laser welding.

Test number	Pulse duration, D_p (ms)	Pulse frequency, f (Hz)	Welding speed, V (mm/s)	Current, I (A)	Focal length, F_l (mm)
1	6	15	8.3	80	20
2	8	15	6.2	80	20
3	8	15	8.3	80	20
4	8	15	10	80	20
5	10	15	8.3	80	20
6	8	20	8.3	80	15
7	8	10	8.3	80	15
8	8	15	8.3	80	15
9	8	15	8.3	80	25

TABLE II. Parameters of welding in tests 2, 3, and 4.

Test number	D_p (ms)	f (Hz)	I (A)	F_l (mm)	V (mm/s)
2	8	15	80	20	6.2
3	8	15	80	20	8.3
4	8	15	80	20	10

A. Process parameter effects on temperature distribution

1. Welding speed effect

In order to investigate the effect of welding speed on the temperature field near the molten pool of Ti6Al4V (in tests 2, 3, and 4), the speed of welding was varied while keeping other parameters constant. These parameter values are given in Table II.

As can be seen in Fig. 3, the maximum temperature measured by the thermocouple clearly increased from 113 to 162 °C as the welding speed reduced from 10 to 6.2 mm/s. It shows that changing the welding speed has had a direct relationship with Ti6Al4V alloy surface interaction. Although the speed was changed about 40%, the temperature varied about 30%. To explain this phenomenon, it can be said that as the welding speed decreases, the laser beam interaction conditions varied with the interface bonding condition between PET and Ti6Al4V. As a result, more heat is generated due to the increased time of the reaction between the surface and the beam, the size of bobbles has increased by time duration in laser

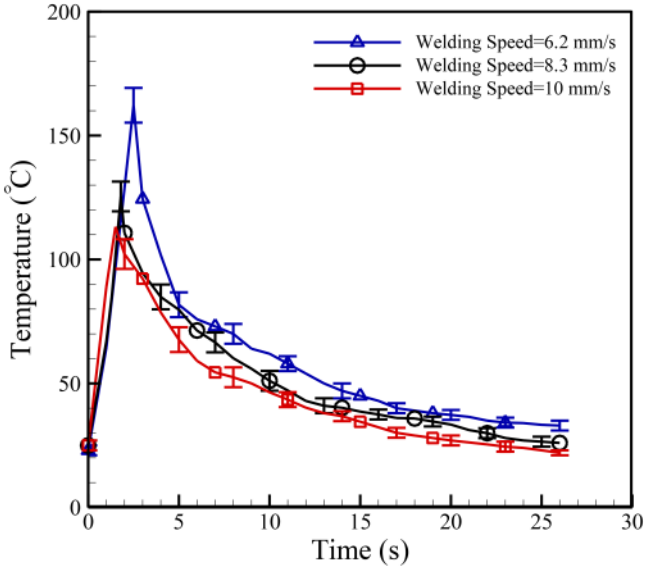

FIG. 3. Temperature field vs time as a function of welding speed.

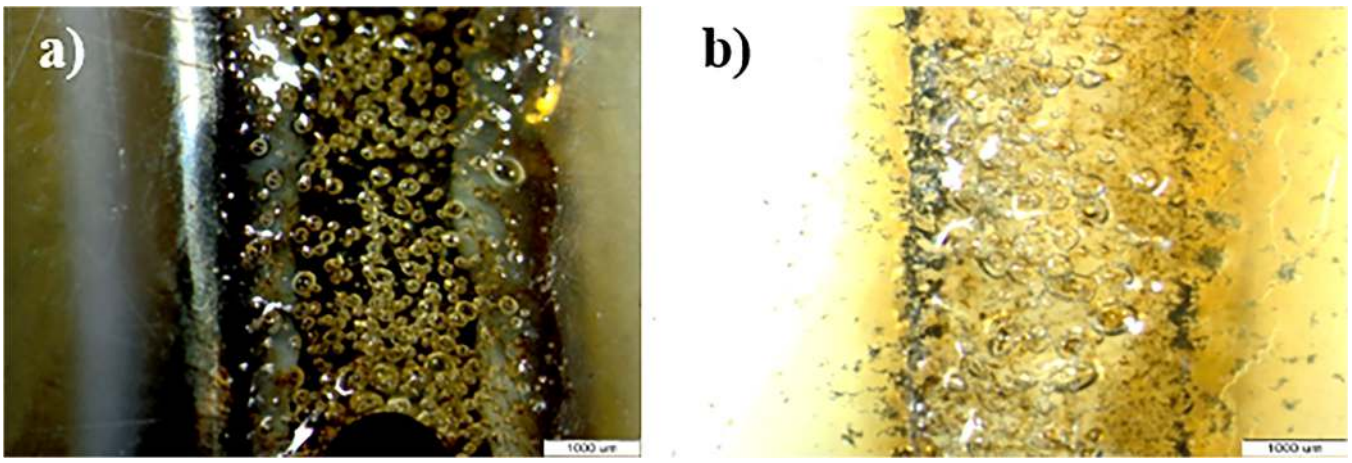

FIG. 4. Effect of welding speed on HAZ, shape, and the number of bubbles, (a) $V = 6.2$ mm/s and (b) $V = 8.3$ mm/s.

bonding process, as shown in Fig. 4. Hence, the rate of increasing temperature is not an exact linear relation to welding speed variation.

Figure 4 shows a comparison of HAZ and bubbles created in the joint between PET and titanium in tests 2 and 3. Bubbles are gases trapped in the molten pool during welding.

Moreover, the width of the HAZ region vividly decreased as the welding speed increased. Apart from this, a comparison of Figs. 4(a) and 4(b) shows that the number of bubbles increased in Fig. 4(a) at a lower speed. Furthermore, the shapes and distribution of the bubbles are more regular in Fig. 4(a) than in Fig. 4(b). An increase in the number of bubbles due to increased gas solubility and as a result of enhancing the temperature is logical. This is so obvious that the extension of the bubble formation region is clearly bigger in Fig. 4(a) due to more heat dissipation through the interface region between PET and the Ti6Al4V alloy surface. The increase in the number of bubbles in the weld reduces the contact surface of the joint of the titanium alloy and PET, thus reducing the weld strength.

2. Pulse duration effect

The laser parameters used to study the effects of pulse duration on temperature distribution and the number of bubbles in tests 1, 3, and 5 are given in Table III.

TABLE III. Parameters of welding in tests 1, 3, and 5.

Test number	D_p (ms)	f (Hz)	I (A)	F_1 (mm)	V (mm/s)
1	6	15	80	20	8.3
3	8	15	80	20	8.3
5	10	15	80	20	8.3

In Fig. 5, temperature distribution versus time at different pulse durations for the titanium alloy is shown. As observed in Fig. 5, increasing the pulse duration from 6 to 10 ms clearly increases the heating cycle, which, in turn, significantly increases the bubble numbers. Not only are the samples subject to higher temperatures (the maximum temperature of the sample at a distance of 2 mm from the weld center is increased from 71 to 143 °C), more laser line energy increases the number of bubbles instead of increasing the dimensions of the bubbles. For this reason, it can be said that increasing the pulse energy by enhancing the pulse duration, more energy is emitted on the interface of the

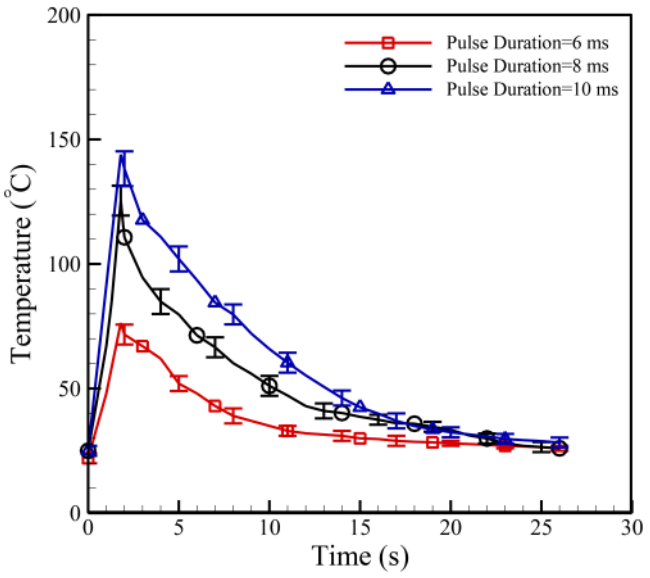

FIG. 5. Temperature distribution vs time as a function of pulse duration.

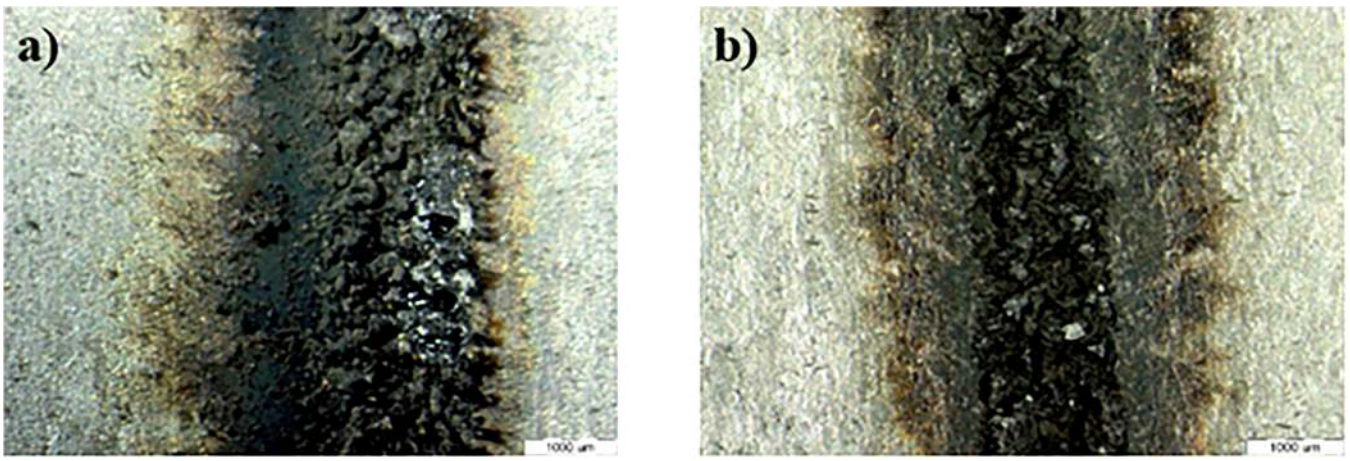

FIG. 6. Effect of pulse duration on weld width and heat affected zone, (a) D_P = 6 ms and (b) D_P = 10 ms.

metal surface and PET, and more heat is generated in the sample. Moreover, the operation time of the laser at a constant pulse frequency increases, and more energy is applied to the sample. The combined effect of these two factors considerably increases the temperature in the titanium alloy.

Figure 6 shows a comparison of the weld width and HAZ at pulse durations of 6 and 10 ms. As can be seen, when the pulse duration rises, more energy is transferred to the samples per time (bigger heating cycle), and, thereby, the weld width and the HAZ of the interface region are expanded. Moreover, the increase in temperature due to the increase in the pulse duration in turn, increases the number of bubbles on the PET plate, which can have a negative effect on the weld strength (see Fig. 7). Also, the width of the bonding region between the metal and the PET interface is clearly wider for a 10 ms pulse duration due to the higher time taken for heat to dissipate into the wider area near the melt pool. It can be said that increasing the pulse duration evidently increases the width of the molten area at the interface region of PET and the Ti6Al4V alloy surface. In this region, no bubble is observed because of the lower intensity of laser beam density.

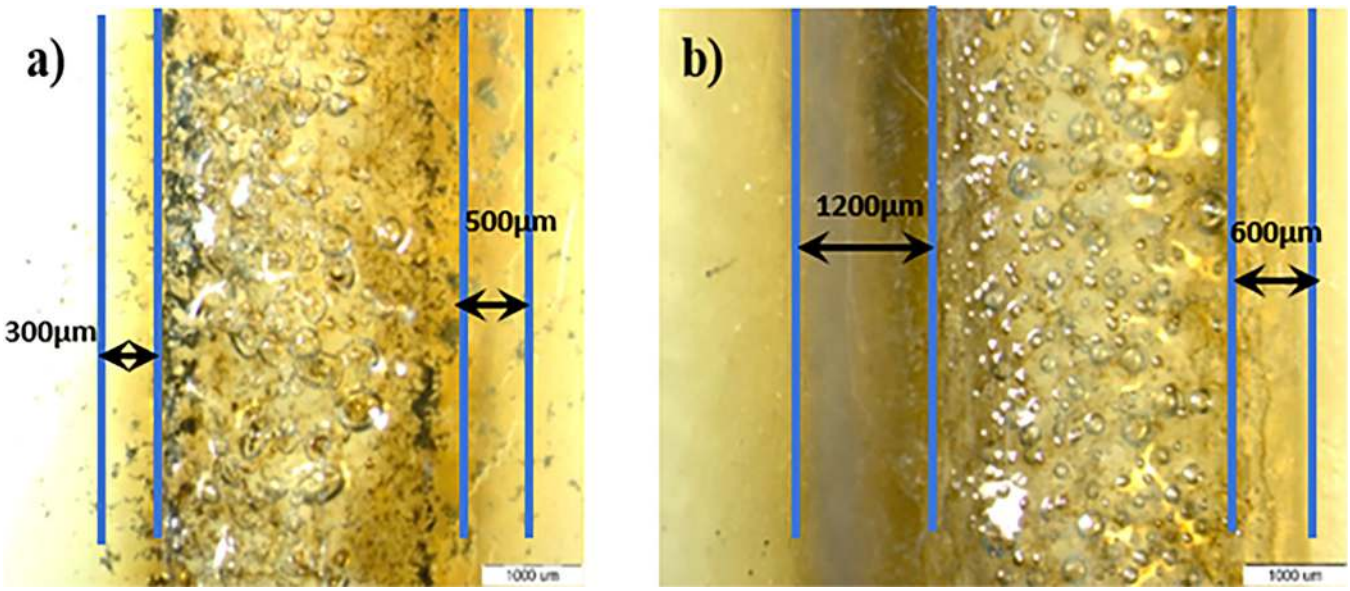

FIG. 7. The effect of pulse duration on the shape and number of bubbles, (a) D_P = 6 ms and (b) D_P = 10 ms.

TABLE IV. Parameters of welding in tests 8 and 3.

Test number	D_p (ms)	f (Hz)	I (A)	F_l (mm)	V (mm/s)
8	8	15	80	15	8.3
3	8	15	80	20	8.3

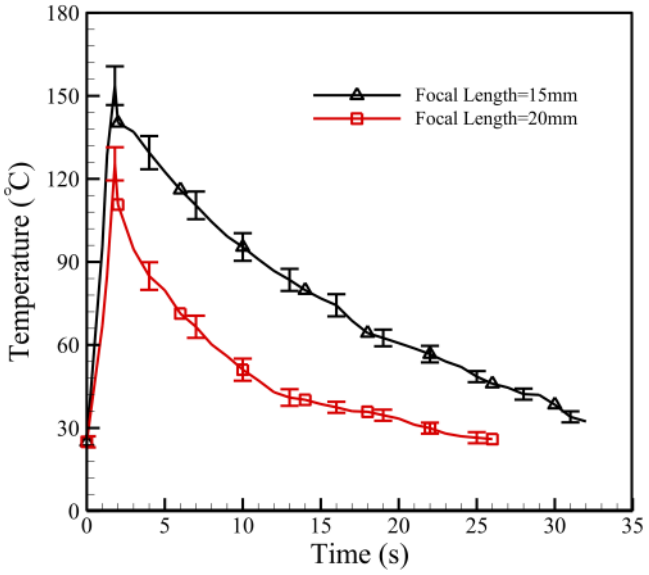

FIG. 8. Temperature distribution vs time as a function of focal length.

3. Focal length effect

The laser parameters used to study the effects of focal length on temperature distribution and the number of bubbles in tests 8 and 3 are given in Table IV.

Figure 8 shows that the thermocouple-recorded temperature increases by approximately 30 °C as the focal length reduces from 20 to 15 mm. For this phenomenon, it can be said that when laser parameters, such as power and frequency and other conditions, are kept constant, and as the focal length reduces and the effect of the laser beam spot becomes smaller, the energy density of the laser beam rises. When the energy density rises, more heat is generated and the weld temperature increases.

As can be seen in Fig. 9, with a higher laser focus and higher energy given to the titanium alloy and the PET samples at low focal lengths, the temperature increases, and the bubbles lose their spherical shape and appear in the form of irregular shapes [Fig. 9(a)]. The shape variation of bubbles can affect PET strength in welding, and the shape of bubbles influences the stress distribution of the joint. Therefore, it can be said that a change in the focal length noticeably affects the quality and strength of welding.

B. Molten pool characterization

It is observed in Fig. 10 that the molten pool is formed in the titanium alloy by considering a low mean laser power used in conduction mode welding. Also, the keyhole phenomenon is not observed in the molten pool.

The molten pool size results of samples 1, 3, and 5 (pulse duration variations) are given in Table V. Because the laser power and the heat generation increase when the pulse duration rises, the

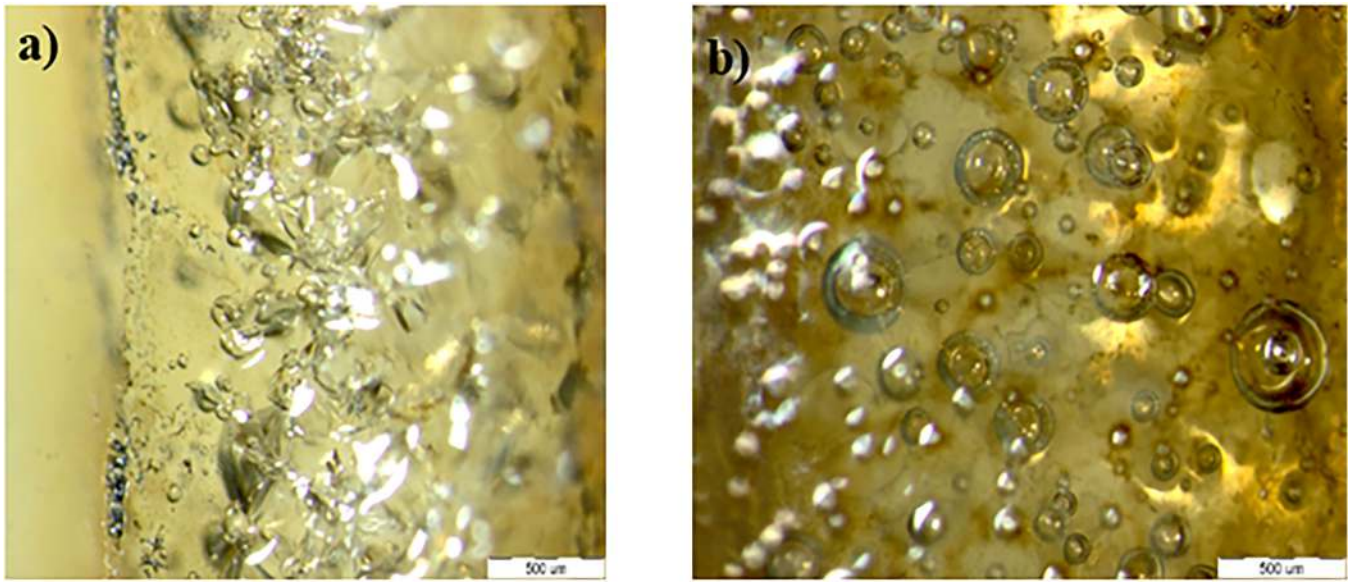

FIG. 9. The effect of focal length on the shape and number of bubbles, (a) F_l = 15 mm and (b) F_l = 20 mm.

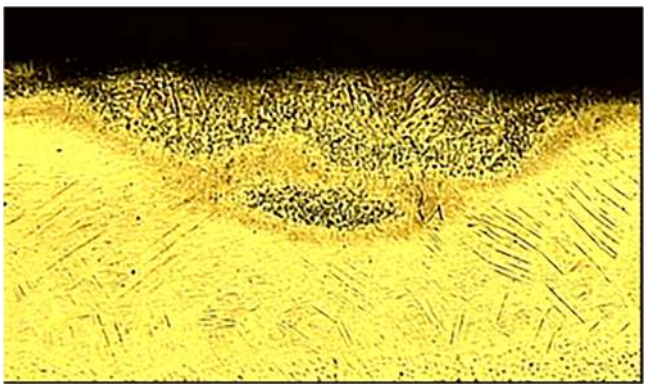

FIG. 10. Microstructure of the Ti6Al4V fusion zone.

TABLE V. Geometry of the Ti6Al4V melt pool at different pulse durations.

Test number	Pulse duration (ms)	Melt pool width (μm)	Melt pool depth (μm)
1	6	230	100
3	8	280	145
5	10	320	190

depth and the width of the molten pool have an increasing trend. For these samples, the increasing width and depth trends have been demonstrated in Figs. 11(a) and 11(b). The increase in the depth and width of the molten pool has had an identical trend at the conduction mode for the Ti6Al4V alloy.

C. Effect of parameters on shear load

The effects of pulse duration and focal length on the shear load have been investigated so as to determine the effects of variation of these parameters on the mechanical strength of the joint. As shown in Fig. 12, upon increasing the pulse duration, the shear load first increased from 30 to 55 N and then reduced by about 10% upon an excessive increase of pulse duration. This is because of the augmentation of the number of bubbles when the pulse duration was increased from 8 to 10 ms; the shear load decreased, although the width of HAZ increased. It could be said that decreasing the bonding surface between PET and the Ti6Al4V alloy due to increasing the number and dimension of bubbles has been more effective than increasing the width of HAZ.

Variation of the focal length has had more effect on the shear load than on the pulse duration. As observed in Fig. 13, increasing the focal length from 15 to 20 mm has decreased the laser beam energy density, thereby preventing a piercing of the PET at the bonding area. This level of energy acts as a thresholding boundary to produce a safe joint. A further increase of the focal length from 20 to 25 mm clearly reduces the energy density and as a result decreases the shear load and width of the HAZ region by about

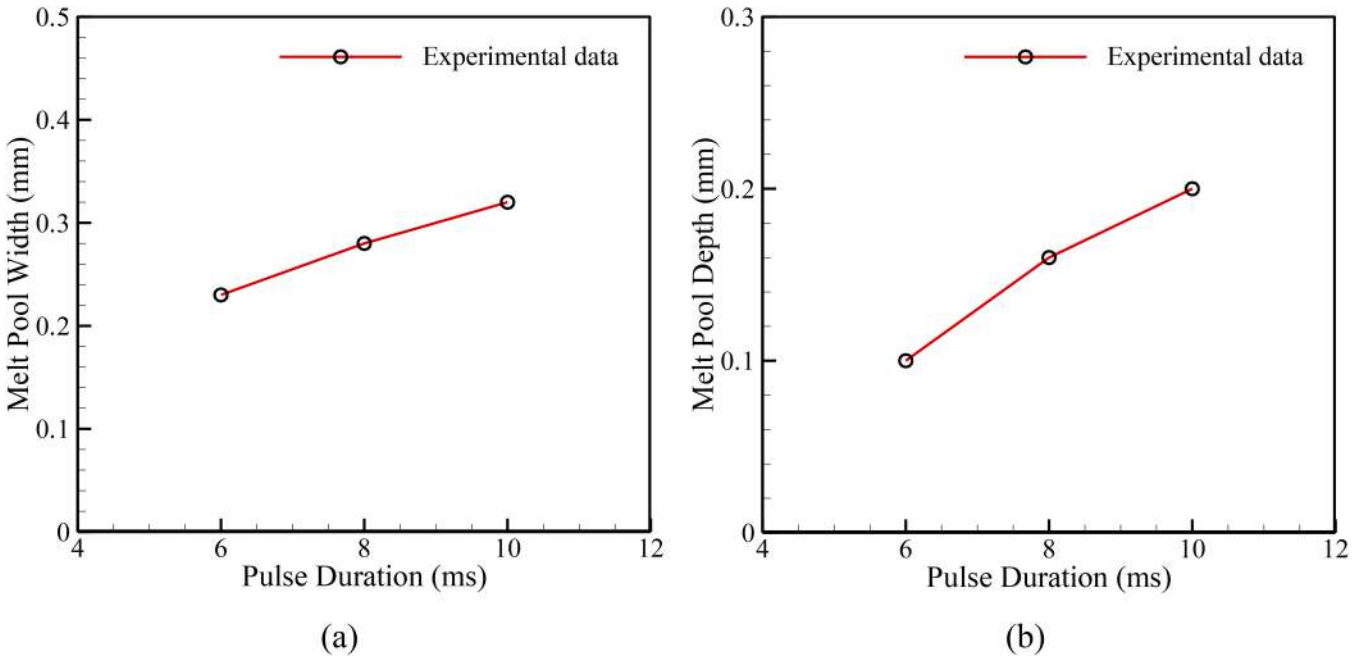

FIG. 11. The variations of melt pool dimensions vs pulse duration for (a) melt pool width and (b) melt pool depth.

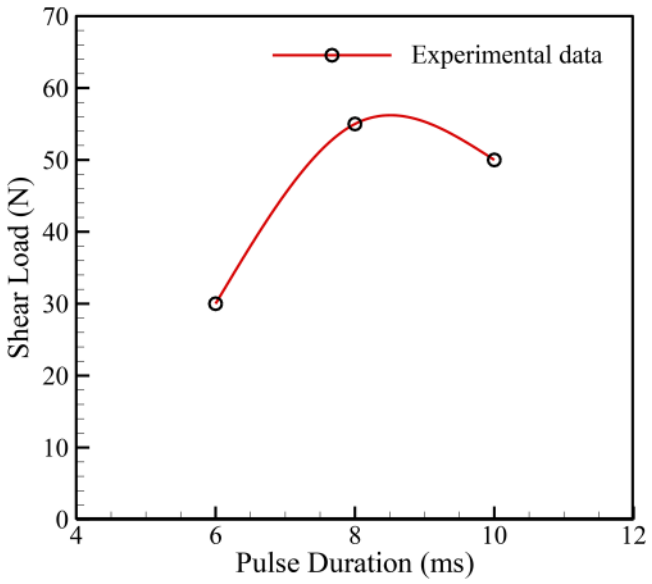

FIG. 12. The effect of pulse duration on shear load.

40%, which, in turn, leads to more significant diminishment than when increasing the pulse duration. It can be concluded that focal length exercises a major influence on the mechanical strength of the joint.

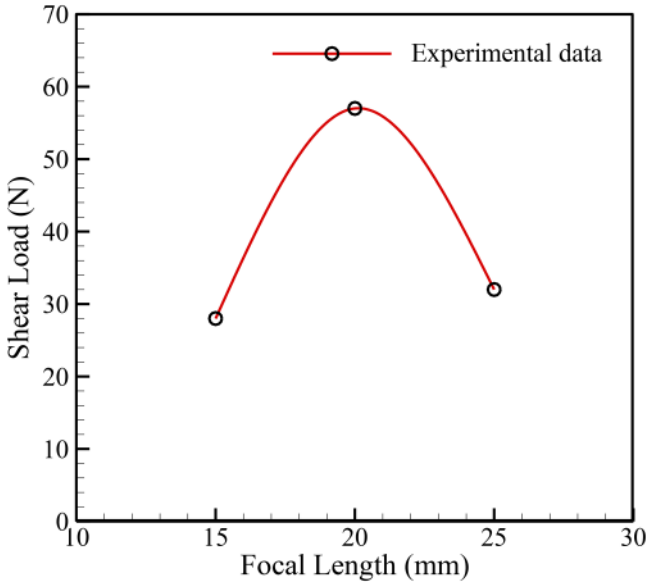

FIG. 13. The effect of focal length on shear load.

IV. CONCLUSION

- According to the temperature field and metallography results, the molten pool's microstructure containing α and β phases proves that the molten pool had high heating and cooling rates.
- Because PET completely melted and a distinct area formed in the laser spot in high power welding, PET and Ti6Al4V could be welded only at low laser powers; otherwise, no proper joint could be created.
- Investigating the temperature field indicated that welding at low focal lengths increases the likelihood of complete PET sheet melting and makes it impossible to create a proper joint due to the low melting point of PET.
- The titanium surface temperature increased as the welding speed increased since the time of the reaction between the laser beam and the titanium alloy increased.
- The increase of the welding speed provided regular bubble shapes and a uniform distribution of bubbles in the PET/titanium joint.
- By an increase in the pulse duration and thus the increased pulse energy, the titanium sample's temperature rose. Also, the number of generated bubbles increased.
- Reducing the focal length changed the regular spherical shape of bubbles. Therefore, given that a low focal length prevented proper welding, it can be said that the focal length has a key role to play in the variation of the shear load between PET and a titanium joint. The shear load had a variation about 40% in comparison with the only 10% for pulse duration.
- The welding speed in the range of 8–10 mm/s and the focal length in the range of 15–20 mm can produce acceptable joint quality. The welding speed and the focal length have had a remarkable effect on the bonding quality.

ACKNOWLEDGMENTS

This work was supported by Hubei superior and distinctive discipline group of "Mechatronics and Automobiles" and Hubei Natural Science Foundation Youth Project (No. 2020CFB320).

REFERENCES

[1]D. Gu, M. Guo, H. Zhang, Y. Sun, R. Wang, and L. Zhang, "Effects of laser scanning strategies on selective laser melting of pure tungsten," Int. J. Extreme Manuf. **2**, 025001 (2020).
[2]G. Djogo, J. Li, S. Ho, M. Haque, E. Ertorer, J. Liu, X. Song, J. Suo, and P. R. Herman, "Femtosecond laser additive and subtractive micro-processing: Enabling a high-channel-density silica interposer for multicore fibre to silicon-photonic packaging," Int. J. Extreme Manuf. **1**, 045002 (2019).
[3]R. Tino, M. Leary, A. Yeo, E. Kyriakou, T. Kron, and M. Brandt, "Additive manufacturing in radiation oncology: A review of clinical practice, emerging trends and research opportunities," Int. J. Extreme Manuf. **2**, 012003 (2020).
[4]J. Ding, G. Yu, C. Fang, J. Wang, R. Zheng, B. Li, J. Zhou, X. Zhu, and W. Wei, "High beam quality of nanosecond Nd:YAG slab laser system with SBS-PCM," Opt. Commun. **475**, 126273 (2020).
[5]W. Wang, W. Wu, S. Wu, Y. Li, C. Huang, X. Tian, X. Fei, and J. Huang, "Adhesive-free bonding homogenous fused-silica Fabry–Perot optical fiber low pressure sensor in harsh environments by CO_2 laser welding," Opt. Commun. **435**, 97–101 (2019).

[6]L. Mei, D. Yan, G. Chen, Z. Wang, and S. Chen, "Influence of laser beam incidence angle on laser lap welding quality of galvanized steels," Opt. Commun. **402**, 147–158 (2017).
[7]C. Li, K. Wang, and J. Huang, "Simulation of the effect of spot size on temperature field and weld forming in laser tissue welding," Optik **155**, 315–323 (2018).
[8]H. C. Chen, F. L. Ng, and Z. Du, "Hybrid laser-TIG welding of dissimilar ferrous steels: 10 mm thick low carbon steel to 304 austenitic stainless steel," J. Manuf. Process. **47**, 324–336 (2019).
[9]S. F. Chua, H. C. Chen, and G. Bi, "Influence of pulse energy density in micro laser weld of crack sensitive Al alloy sheets," J. Manuf. Process. **38**, 1–8 (2019).
[10]S. Yan and Y. Shi, "Influence of laser power on microstructure and mechanical property of laser-welded Al/Cu dissimilar lap joints," J. Manuf. Process. **45**, 312–321 (2019).
[11]G. Chandrasekar, C. Kailasanathan, and M. Vasundara, "Investigation on un-peened and laser shock peened dissimilar weldments of Inconel 600 and AISI 316L fabricated using activated-TIG welding technique," J. Manuf. Process. **35**, 466–478 (2018).
[12]G. Casalino, A. Angelastro, P. Perulli, C. Casavola, and V. Moramarco, "Study on the fiber laser/TIG weldability of AISI 304 and AISI 410 dissimilar weld," J. Manuf. Process. **35**, 216–225 (2018).
[13]K. D. Ramkumara, S. P. Dev, K. V. Prabhakar, R. Rajendran, K. G. Mugundan, and S. Narayanan, "Microstructure and properties of Inconel 718 and AISI 416 laser welded joints," J. Manuf. Process. **266**, 52–62 (2019).
[14]G. Kelly, "Quasi-static strength and fatigue life of hybrid (bonded/bolted) composite single-lap joints," Compos. Struct. **72**, 119–129 (2006).
[15]A. Mian, G. Newaz, L. Vendra, and N. Rahman, "Laser bonded microjoints between titanium and polyimide for applications in medical implants," J. Mater. Sci. **16**, 229–237 (2005).
[16]Z. Gui, G. Min, D. Liu, and P. Hu, "Double-sided laser welding of dissimilar titanium alloys with linear variable thickness," Int. J. Adv. Manuf. Technol. **79**, 1597–1606 (2015).
[17]R. M. Miranda, E. Assunção, R. J. Silva, J. P. Oliveira, and L. Quintino, "Fiber laser welding of NiTi to Ti-6Al-4V," Int. J. Adv. Manuf. Technol. **81**, 1533–1538 (2015).
[18]J. Pouquet, R. M. Miranda, L. Quintino, and S. Williams, "Dissimilar laser welding of NiTi to stainless steel," Int. J. Adv. Manuf. Technol. **61**, 205–212 (2012).
[19]M. Balasubramanian, "Characterization of diffusion-bonded titanium alloy and 304 stainless steel with Ag as an interlayer," Int. J. Adv. Manuf. Technol. **82**, 153–162 (2016).
[20]C. Tan, X. Song, S. Meng, B. Chen, L. Li, and J. Feng, "Laser welding-brazing of Mg to stainless steel: Joining characteristics, interfacial microstructure, and mechanical properties," Int. J. Adv. Manuf. Technol. **86**, 203–213 (2016).
[21]A. Yıldız, Y. Kaya, and N. Kahraman, "Joint properties and microstructure of diffusion-bonded grade 2 titanium to AISI 430 ferritic stainless steel using pure Ni interlayer," Int. J. Adv. Manuf. Technol. **86**, 1287–1298 (2016).
[22]Y. Zhang, D. Q. Sun, X. Y. Gu, and Y. J. Liu, "Nd/YAG pulsed laser welding of TC4 titanium alloy to 301L stainless steel via pure copper interlayer," Int. J. Adv. Manuf. Technol. **90**, 953–961 (2017).
[23]N. Kumar, M. Mukherjee, and A. Bandyopadhyay, "Study on laser welding of austenitic stainless steel by varying incident angle of pulsed laser beam," Opt. Laser Technol. **94**, 296–309 (2017).
[24]T. A. Mai and A. C. Spowage, "Characterisation of dissimilar joints in laser welding of steel–kovar, copper–steel and copper–aluminium," Mater. Sci. Eng. A **374**, 224–233 (2004).
[25]M. Speka, S. Matteï, M. Pilloz, and M. Ilie, "The infrared thermography control of the laser welding of amorphous polymers," NDT E Int. **41**, 178–183 (2008).
[26]M. Akbari, S. Saedodin, D. Toghraie, R. Shoja-Razavi, and F. Kowsari, "Experimental and numerical investigation of temperature distribution and melt pool geometry during pulsed laser welding of Ti6Al4V alloy," Opt. Laser Technol. **59**, 52–59 (2014).
[27]M. R. Frewin and D. A. Scott, "Finite element model of pulsed laser welding," Weld. J. **78**, 15-s–22-s (1999).
[28]F. Kong, S. Santhanakrishnan, D. Lin, and R. Kovacevic, "Modeling of temperature field and grain growth of a dual phase steel DP980 in direct diode laser heat treatment," J. Mater. Process. Technol. **209**, 5996–6003 (2009).
[29]A. H. Faraji, M. Goodarzi, S. H. Seyedein, and C. Maletta, "Effects of welding parameters on weld pool characteristics and shape in hybrid laser-TIG welding of AA6082 aluminum alloy: numerical and experimental studies," Weld. World **60**, 137–151 (2016).
[30]K. Abderrazak, S. Bannour, H. Mhiri, G. Lepalec, and M. Autric, "Numerical and experimental study of molten pool formation during continuous laser welding of AZ91 magnesium alloy," Comput. Mater. Sci. **44**, 858–866 (2009).
[31]M. Akbari, S. Saedodin, A. Panjehpour, M. Hassani, M. Afrand, and M. J. Torkamany, "Numerical simulation and designing artificial neural network for estimating melt pool geometry and temperature distribution in laser welding of Ti6Al4V alloy," Optik **127**, 11161–1172 (2016).
[32]D. Jiang, A. S. Alsagri, M. Akbari, M. Afrand, and A. A. Alrobaian, "Numerical and experimental studies on the effect of varied beam diameter, average power and pulse energy in Nd: YAG laser welding of Ti6Al4V," Infrared Phys. Technol. **101**, 180–188 (2019).
[33]M. Azizpour, M. Ghoreishi, and A. Khorram, "Numerical simulation of laser beam welding of Ti6Al4V sheet," J. Comput. Appl. Res. Mech. Eng. **4**, 145–154 (2015).